Tunable Bandwidth for Application-specific SAxP process enhancement

Paolo Alagna[a], Will Conley[b], Greg Rechtsteiner[b],

Kathleen Nafus[c] , Serge Biesemans[c]

Gian Francesco Lorusso[d]

a) Cymer LLC, Kapeldreef 75, 3001 Leuven, Belgium
b) Cymer LLC, 17075 Thornmint Court, San Diego, CA 92127
c) TEL, resident at imec, Kapeldreef 75, 3001 Leuven, Belgium
d) IMEC, Kapeldreef 75, 3001 Leuven, Belgium

ABSTRACT

Use of ArFi lithography requires Application-specific tuning to maximize patterning process windows. Previous investigations into the effects of light source bandwidth on imaging performance have provided the foundation for this work by identifying significant improvements in Exposure Latitude for reduced sensitivity to dose variations.
This study will focus on the increase in image contrast that 200 fm light source E95 bandwidth enables on Self-Aligned Quadruple Patterning (SAQP) block and core features and Self-Aligned Double Patterning (SADP) core features. Focus of our investigation will be the understanding of roughness and profile variation through different exposure conditions.

INTRODUCTION

Lithographers have enabled the continued scaling of semiconductor devices down to the 7 nm node by using ArF immersion DUV and multiple pattering (SAxP) methods. This achievement has necessitated the use of all adjustable parameters to ensure that transistor-level variability is minimized. For example, critical dimension uniformity (CDU) and pattern placement / fidelity variability must be minimized to ensure device performance.

As a result, the contributions of line-edge roughness (LER) and line-width roughness (LWR) to CDU are of concern as part of the larger Edge Placement Error (EPE) budget for advanced devices. The typical contributors to DUV patterning LWR are image contrast[1-3], resist chemistry and processing[4-5], and etch transfer effects[6-7]. Prior work has been reported on the impact of the illumination properties on lithographically-printed photoresist patterns[11-13].

In response, Cymer performed multiple studies demonstrating that improvements in on wafer, printed feature roughness and pattern fidelity can be achieved for 2D features using lower light source bandwidth[14-16]. Specifically, the study presented at SPIE in 2017 provided a deeper understanding of the key performance indicator (KPI) response of regular matrixes of pillars (patterned using PTD process) and holes (defined through an NTD process). As summarized in Table 1, the on wafers results show that CDU and pattern fidelity KPIs were improved when low bandwidth (high contrast) conditions were used.

Description	Image	Process Window	CD Uniformity change	Pattern Placement Error 3σ change
Pillars ADI CD (nm) = 41 ± 3 (Litho PTD process)	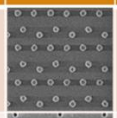	ΔDOF = +30 nm ΔEL = +1 %	-0.1 nm (LCDU)	up to -0.2 nm
Trenches AEI CD (nm) = 24/32 ± 3 (Litho NTD process)	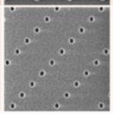	ΔDOF = 0 nm ΔEL = +4 %	-0.2 nm (FOV_CDU)	na

***Note** : Between 12k and 18k features measured per wafer.*

Table 1. SADP Blocks and SAQP Cuts KPI response.

The target of this work is the conclusion of the study started in 2017[16]. The process flow considered is made by the two patterning solutions reported in Figure 1, both compatible with imec 7 nm process node.

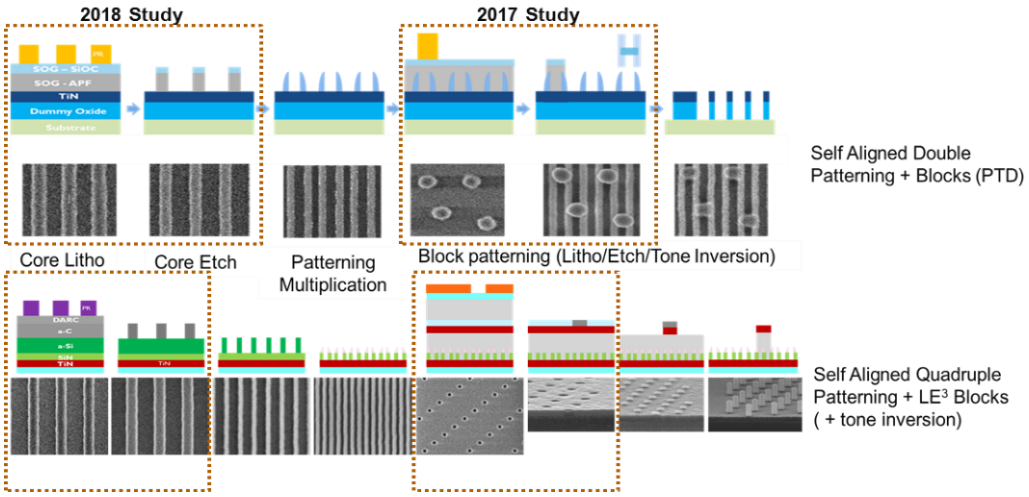

Figure 1. SAxP patterning solutions for the 2017 and 2018 studies.

This study focuses on the application of tunable light source bandwidth on regular line-trenches features. Two different metal core patterns are investigated: M0C is a SADP flow with an ADI target CD of 42 nm at 84 nm pitch; and M1C is a SAQP flow with an ADI target of 51 nm at 128 nm pitch (see Figure 2).

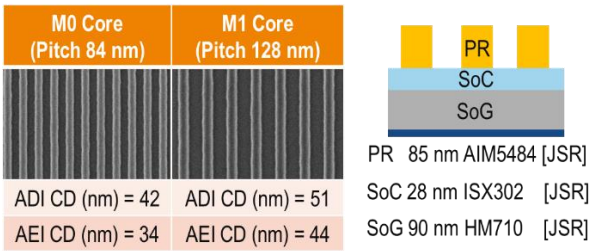

Figure 2. M0 and M1 core features for the 2018 studies.

In addition to the standard KPIs investigated in the previous studies, advanced KPIs (such as analysis of PSD and ξ) are investigated to properly assess the impact on light source bandwidth on short and long-range line roughness. The interest in these advanced KPIs is based on the framework proposed by T. Sandstrom and C. Rydberg[16] for modeling of roughness contributions (see Figure 3).

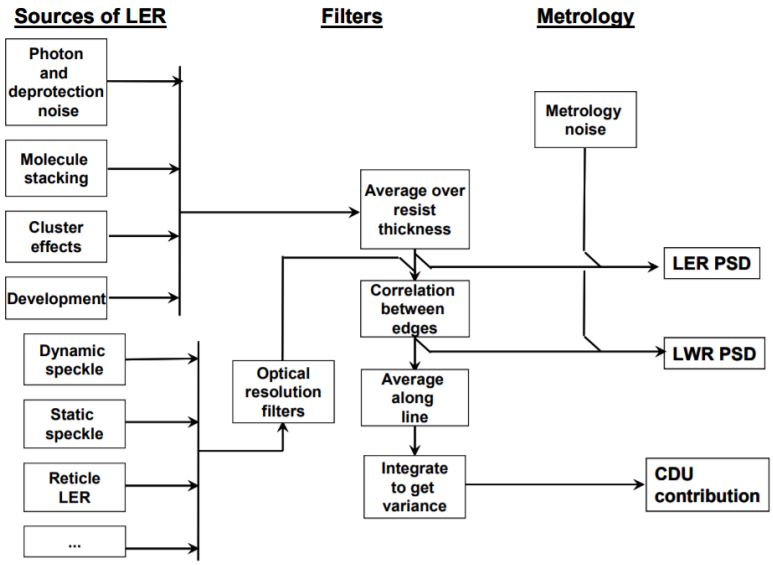

Figure 3. T. Sandstrom and C. Rydberg proposed framework[16].

This framework provides a clear summary of the critical correlations between on wafer KPIs (such as LEW, LWR, and CDU), and can be considered a foundation for studies of light source coherence and speckle on lithographically-printed photoresist patterns[18-19]. Previous Cymer studies[19] reported that a change in light source bandwidth could drive higher temporal coherence, as temporal coherence is fundamentally linked to laser bandwidth (see Figure 4).

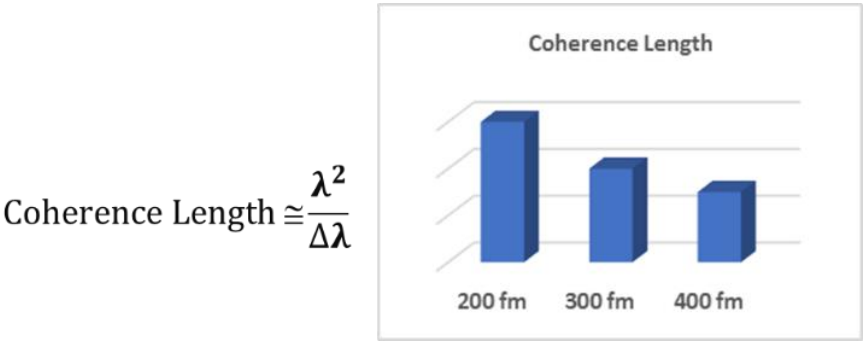

Figure 4. Coherence length and its dependency to bandwidth[19].

The aforementioned studies indicate that lower light source bandwidth may degrade line roughness; therefore, this study also focuses on assessing the short and long-range roughness performance of two SAxP line (core) processes as a function of light source bandwidth.

EXPERIMENTAL DETAILS AND RESULTS

For the experiments in this study, the dose to size is defined through the exposure of the classic focus exposure matrix (FEM) keeping as reference the ADI targets reported in the introduction and a tolerance of ± 2 nm. The process window is measured using steps of 0.5 mJ/cm^2 in dose and 30 nm in focus and the other KPIs which are analyzed in this paper have been exposed at the best dose. Different considerations must be made for what is concerning the CD-SEM metrology, because, as it will be described in the following sessions, not all lithography performance indicator can be correctly measured without an optimization of the metrology settings.

Feature	E95% (fm)	Dose (mJ/cm^2)	Dose Step (FEM) (mJ/cm^2)	Focus (µm)	Focus Step (FEM) (µm)	Source
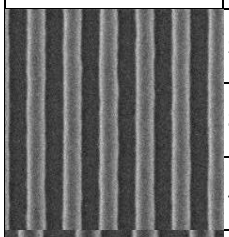	200 fm	18.0	0.5	0.038	0.03	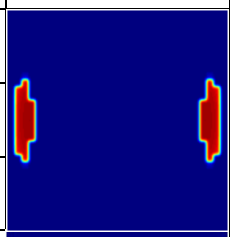
	300 fm	17.9	0.5	0.038	0.03	
	400 fm	18.2	0.5	0.038	0.03	
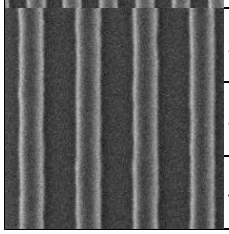	200 fm	17.5	0.5	0.059	0.03	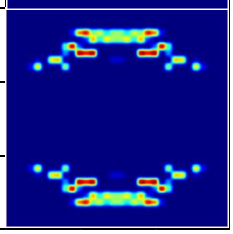
	300 fm	17.3	0.5	0.059	0.03	
	400 fm	17.4	0.5	0.051	0.03	

Table 2. Dose and Focus targeting details, and illumination conditions, for M0C (upper) and M1C (lower).

In this work the original illumination sources for the imec process flows are used to mimic the original process conditions.

The adjectives “conventional” and “advanced” are used to distinguish between two types of analyses performed in this study. The Conventional KPIs consist mainly of the pure CD-SEM metrology output, while the Advanced KPIs consist of more detailed data sets (values and images) and require additional analysis and computation that will be described in a later section.

Conventional Key Performance Indicator (KPI) analysis

The data used for process window calculation were collected from different wafer samples exposed at 200, 300, and 400 fm light source bandwidth using the layout and conditions previously described. An average of four measurement points per field was used for the determinations of process window. As shown in Figure 5, both M0C and M1C do not show any significant sensitivity to bandwidth-induced contrast variation due to their iso-focal characteristics.

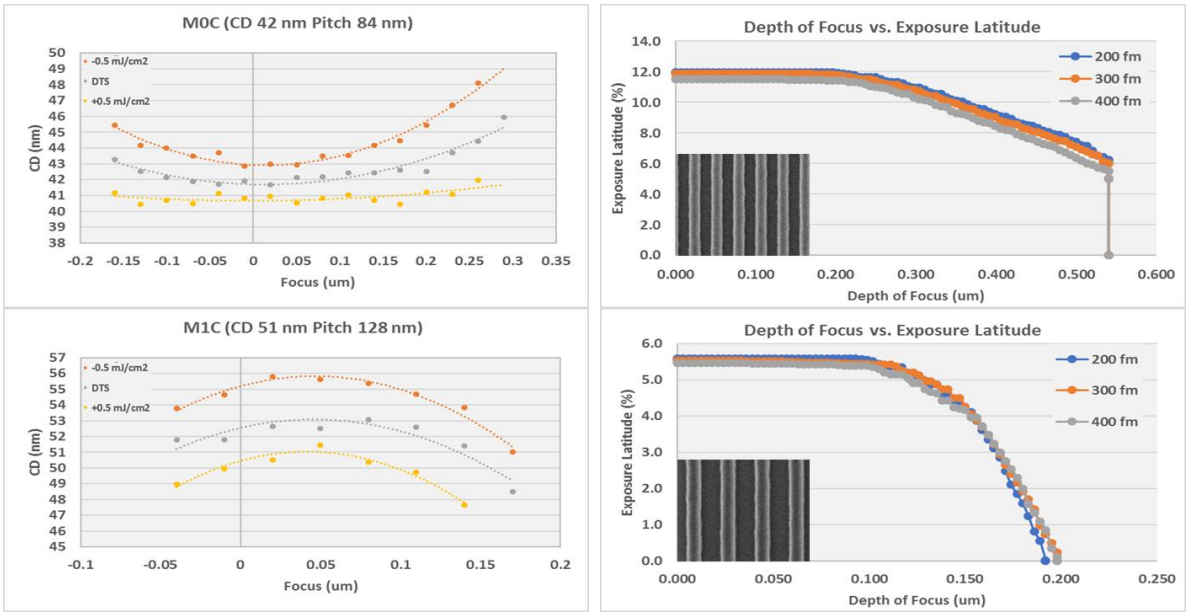

Figure 5. M0 and M1C ADI process windows as a function of light source bandwidth.

The Conventional KPIs also include CD Uniformity (CDU), Line Width Roughness (LWR) and Line Edge Roughness (LER). The CDU is computed as the 3 sigma (by field and by wafer) of the CDs sampled over 10 exposure fields and 40 points per field for a total of 400 measurements per wafer. The LWR and LER values reported are the data directly provided by the CD-SEM used (Hitachi CG63000) at the same sampling level.
Figure 6 shows that besides the expected "smoothing effect" caused by the etch process, there are no significant changes for the three different KPIs as a function of light source bandwidth.

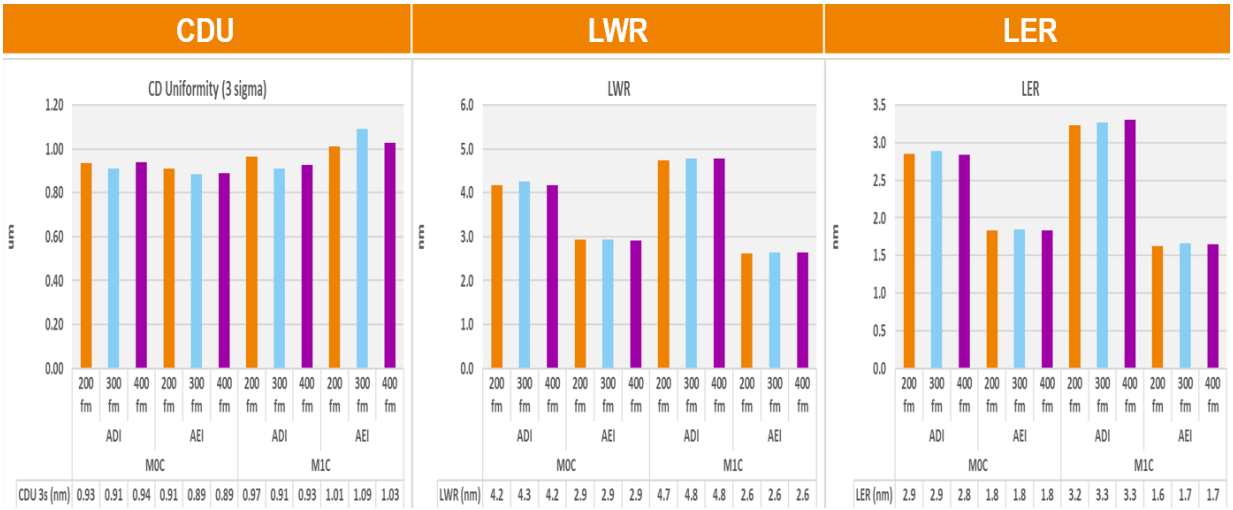

Figure 6. Conventional KPIs as a function of light source bandwidth at ADI and AEI.

Despite these initial results, further study is needed to assess the impact of light source bandwidth on short and long range line roughness which may be of concern to chipmakers.

Advanced Key Performance Indicator (KPI) analysis

To introduce the concept of this study's Advanced KPIs, a simplified sinusoidal based profile will be used. As shown in Figure 7, a sinusoid can be used to representative of three different patterns. Consider how the CD-SEM calculates the roughness (sigma) of each individual pattern: the common roughness sigma value (which is usually the output of the CD-SEM) is by definition the vertical dimension of roughness and gives no information about its spatial complexity. Using that approach, the distribution around the average value would be basically the same ($\sigma_a = \sigma_b = \sigma_c$).

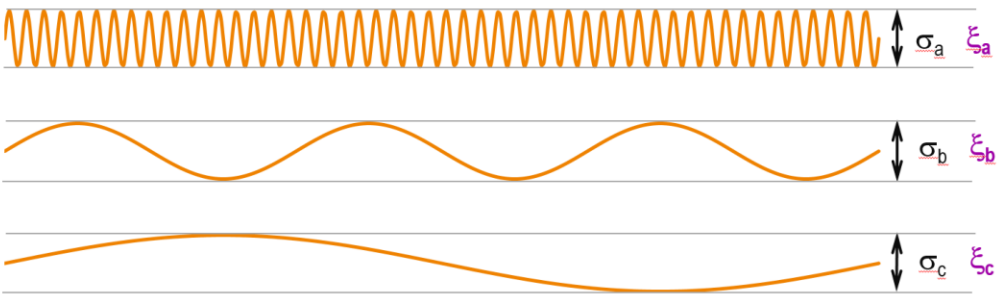

Figure 7. Simplified representation of Advanced KPIs.

To better characterize the spatial complexity of a line edge profile and to determine the dependence of sigma on the length of the measured edge, the correlation length (ξ) factor and the PSD-based LWR analyses must be considered.

Correlation Length [ξ]: the correlation length is defined as follows. Considering the representations in Figure 7 and assume two points *a* and *b* located on the same horizontal plane on the profile's surface; the distance between those two points is *r* (as shown in Figure 8a). For each point, measure the related height (*z*). Compute squared difference in height

for a large number of *a*'s and *b*'s at the same distance *r* and call the average of all those numbers *H(r)*. This is the Height-Height Correlation Function (HHCF). A plot of the different values of *H(r)* as function of *r* results in a chart similar to that reported in Figure 8b.

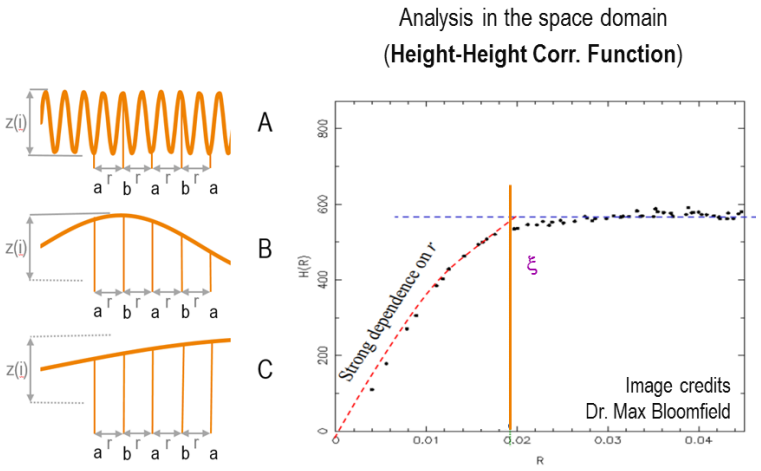

Figure 8. Definition of the Height-Height Correlation Function (HHCF).

Using the simplified representations of Figure 7 the value of the distance *r* can me modulated between *0* and ∞, with the results being grouped in to two different cases.

> *Case 1, r << ξ*: high correlation case. For small *r* distances (*a* and *b are* very close to each other) the value of *H(r)* will be small as well. Therefore, any small change in the distance between the points will be reflected by a change in *H(r)*.
>
> *Case 2, r >> ξ*: low correlation case. For large r distances, the changes between *z(a)* and *z(b)* will not be correlated vertically, since their difference will be an amount based on how much the surface varies vertically.

In other words, as defined by C. Shin[19]: the correlation length means how closely the edge is correlated to its adjacent (neighboring) edge. As the value of the correlation length increases, the adjacent edge is located at a position that is similar to the position at the original edge.

Therefore, it can be concluded that $\sigma_a = \sigma_b = \sigma_c$ while $\xi_a < \xi_b < \xi_c$.

Power Spectral Density (PSD) based LWR measurements: PSD analysis is used to characterize a feature's profile and allows for the extraction of information concerning the LWR (which is basically the area underneath the plot, see Figure 9).

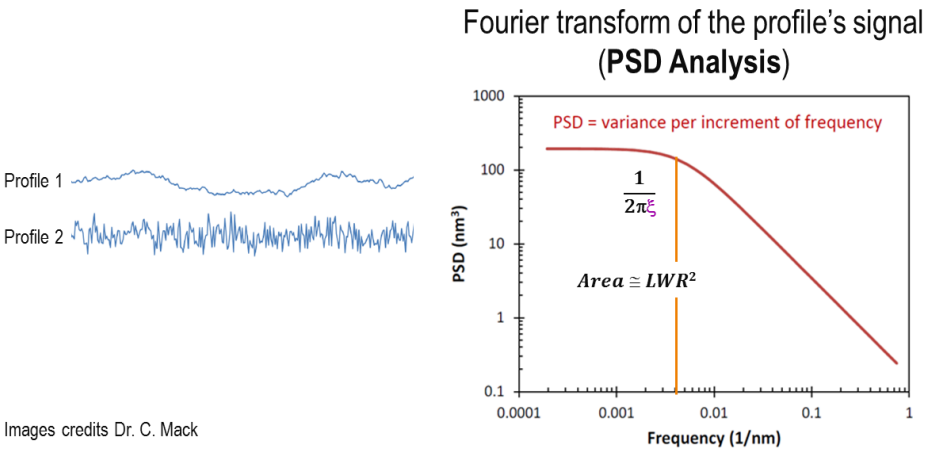

Figure 9. Definition of PSD analysis.

PSD analysis is an image based analysis which requires a certain degree of metrology optimization. This optimization is needed due to the larger FOV which must be balanced with maintaining a good level of image contrast. Table 2 shows the differences in CD-SEM settings between the conventional metric and the PSD-type analysis, and between after lithography and after etch conditions.

Process	M0C CD-SEM Images		M1C CD-SEM Images	
ADI	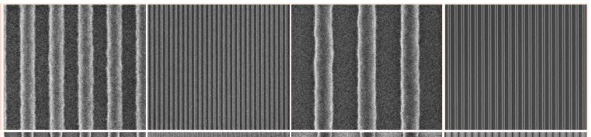			
AEI	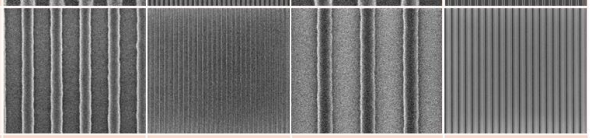			
	PW/CDU/ LWR/LER	PSD	PW/CDU/ LWR/LER	PSD
Acc. Voltage (V)	500 / 800	800 / 800	500 / 800	800 / 800
Probe Current (I)	8	16	8	16
Mag.	300K	50K	300K	50K
Frames	16	32	16	32
Field size (mm)	0.450x0.450	2.7x2.7	0.450x0.450	2.7x2.7
Pixels	512x512	2048x2048	512x512	2048x2048
Pixel size (pxl/nm)	0.88	1.32	0.88	1.32

Table 2: Metrology settings for PSD analysis.

The results of the correlation length (ξ) and PSD analyses are shown in Figures 10 and 11 for the M0C and M1C features, respectively.

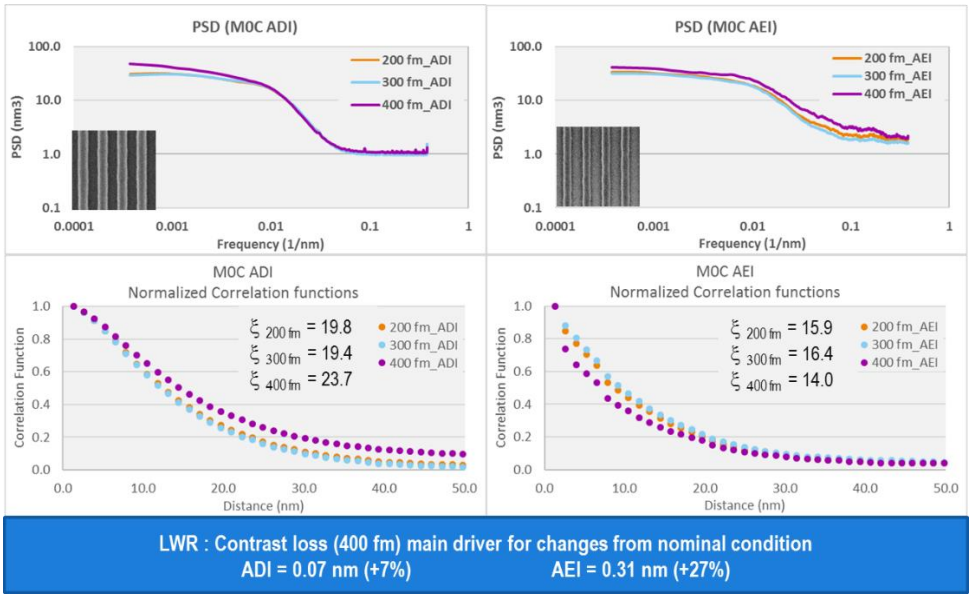

Figure 10. M0C correlation length and PSD analyses.

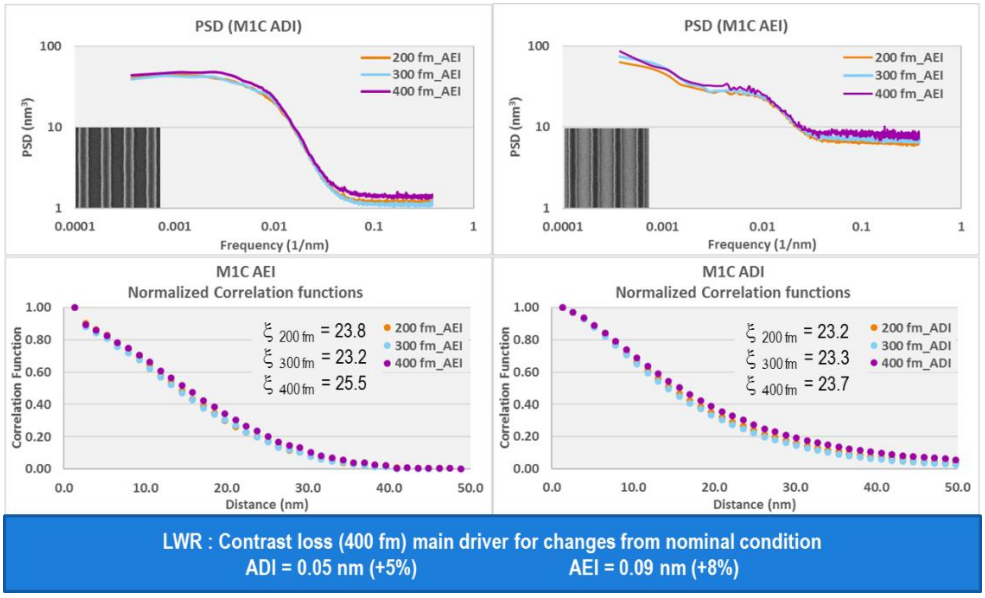

Figure 11. M1C correlation length and PSD analyses.

The analyses show that there are no significant changes in Advanced KPI as a function of lower light source bandwidth (200 fm), while there are incremental signs of changes when higher light source bandwidth (400 fm) is used (likely driven contrast loss).

To further assess the impact of light source bandwidth on the features, long line CDU measurements are made using the following sampling conditions:

- FOV = 0.45 um x 0.45 um
- N. of sequential measures along line = 40
- Total length covered = 18 um
- N. Of exposure fields = 10
- Total number of measurements per wafer = 40

The values of line CD uniformity (3 sigma) are plotted with respect to the dose sensitivity of each feature and exposure condition at ADI and AEI (see Figure 12).

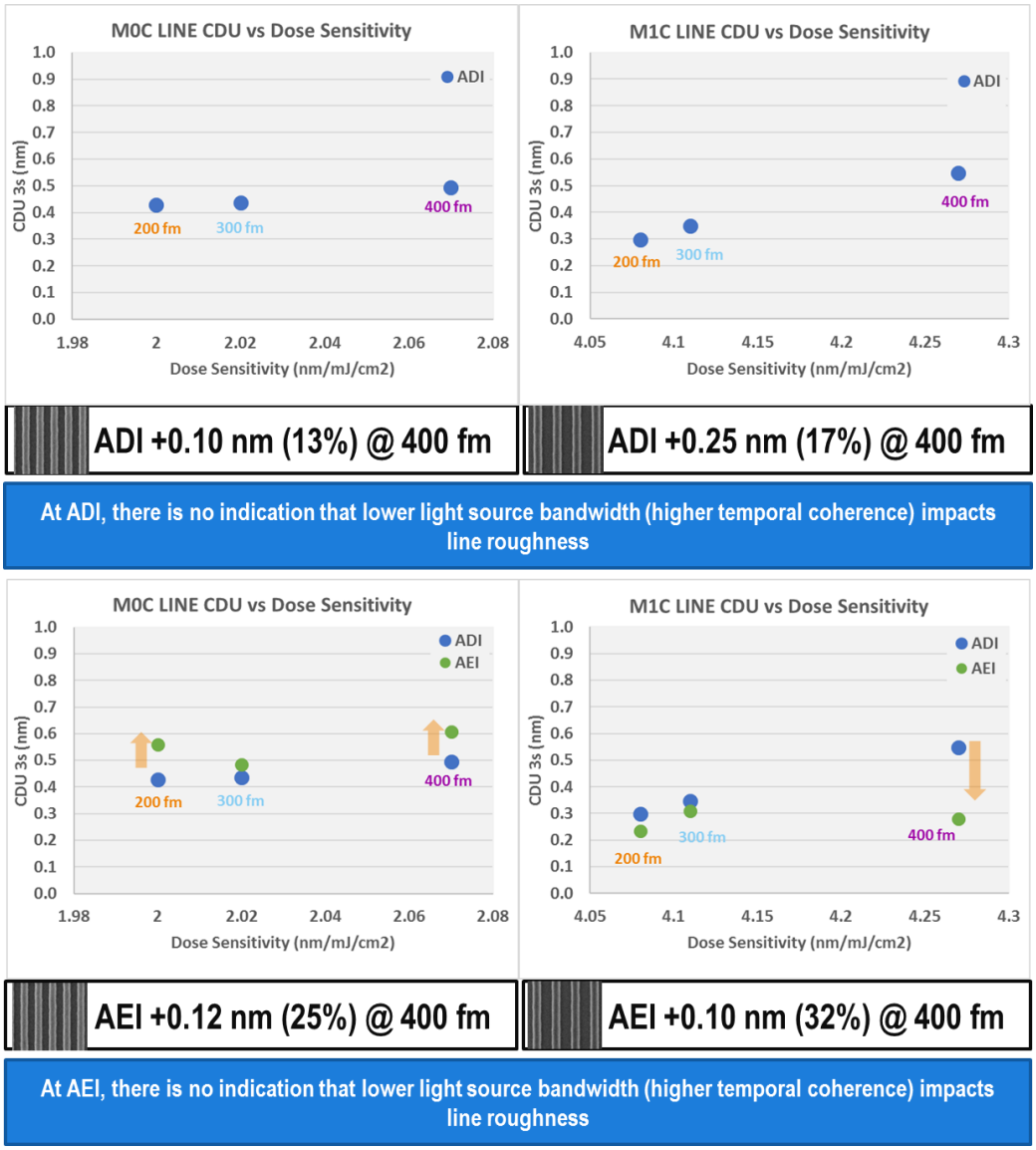

Figure 12. Line CDU as a function of light source bandwidth at ADI and AEI.

While the ADI response matches the expectations based on the PSD and correlation length analyses; the AEI response appears to be modulated by the etch process. The numeric results are summarized in Table 3.

Feature	E95%	Process Window	CDU	LWR	LER	Profile	PSD (LWR)	CDU (18um line)
M0C 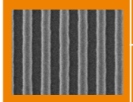	200 fm	ΔEL < 1% ΔDOF < 1%	ADI = 0 nm AEI = 0 nm	ADI = -0.1 nm AEI = 0 nm	ADI = 0 nm AEI = 0 nm	ΔSWA < 1%	ADI = 0 nm AEI = 0 nm	ADI = 0 nm AEI = 0.1 nm
	400 fm		ADI = 0. nm AEI = 0.1 nm	ADI = 0 nm AEI = 0 nm	ADI = 0 nm AEI = 0 nm		ADI = 0 nm AEI = 0.3 nm	ADI = 0.1 nm AEI = 0.1 nm
M1C 	200 fm		ADI = 0.1 nm AEI = 0. nm	ADI = 0 nm AEI = 0 nm	ADI = 0 nm AEI = 0 nm		ADI = 0 nm AEI = -0.1 nm	ADI = 0.1 nm AEI = 0.1 nm
	400 fm		ADI = -0.1 nm AEI = -0.1 nm	ADI = 0 nm AEI = 0 nm	ADI = 0 nm AEI = 0 nm		ADI = 0 nm AEI = 0 nm	ADI = 0.2 nm AEI = 0 nm
Changes vs 300fm < 10%		10% < Changes vs 300fm						

Table 3. Summary of Conventional and Advanced KPI data sets.

CONCLUSIONS

The patterning performance of SAxP core features has been studied as a function of light source bandwidth. Standard KPI analysis shows that the fundamental KPIs of the core features do not vary significantly with the light source E95 bandwidth. Advanced KPI analysis (PSD and long line CDU) results indicate that there is no impact that lower light source bandwidth (higher temporal coherence) impacts line roughness. Further studies into the effects of light source induced dose variation are required to characterize the contribution of the light source to the EPE budget.

ACKNOWLEDGEMENTS

The authors would like to acknowledge the expertise and guidance provided by: Jason Lee, James Bonafede, Simon Hsieh, Yoo Keun Won and Remo Petrella at Cymer; Vito Daniele Rutigliani and Alain Moussa at imec; Marc Demand at TEL; Mircea Dusa and Jan Baselmans at ASML; and Takumichi Sutani, Takeyoshi Ohashi and Yoshikata Takemasa from Hitachi High-Tech.

REFERENCES

[1] W. Hinsberg et al., “Deep-ultraviolet interferometric lithography as a tool for assessment of chemically amplified photoresist performance,” J. Vac. Sci. & Tech. B, vol. 16 (1998).
[2] M. Williamson, A. Neureuther, “Enhanced, quantitative analysis of resist image contrast upon line edge roughness,” Proc. SPIE Adv. Res. Tech. & Proc. XX, 5039, 423 (2003).
[3] A. Pawloski et al., “Characterization of line edge roughness in photoresist using an image fading technique,” Proc. SPIE Adv. Res. Tech. & Proc. XXI, 5376, 414, (2004).
[4] H. Koh et al, “Effect of process parameters on pattern edge roughness of chemically-amplified resists,” Proc. SPIE Adv. Res. Tech. & Proc. XVII, 3999, 240, (2000).
[5] Q. Lin et al., “Line-edge roughness in positive-tone chemically amplified resists: effect of additives and processing conditions,” Proc. SPIE Adv. Res. Tech. & Proc. XVIII, 4345, 78 (2001).
[6] A. Pawloski et al., “The transfer of photoresist LER through etch,” Proc. SPIE Adv. Res. Tech. & Proc. XXIII, 6153, (2006).
[7] T. Wallow et al., “Line-edge roughness in 193-nm resists: lithographic aspects and etch transfer,” Proc. SPIE Adv. Res. Tech. & Proc. XXIII, 6519, (2007).
[8] P. Considme, "Effects of coherence on imaging systems", J. Opt. Soc. Am., Vol 56, No 8 (1966).
[9] L Wang et al., "Speckle reduction in laser projection systems by diffractive optical elements," Appl. Opt., Vol 37, No 10 (1998).
[10] R. Martinsen et al., “Speckle in Laser Imagery: Efficient Methods of Quantification and Minimization,” Proc. LEOS 12th Annual Meeting IEEE, vol 1, Nov (1999).
[11] T. Sandstrom et al., “Dynamic laser speckle in optical projection lithography: causes, effects on CDU and LER, and possible remedies,” Proc. SPIE Adv. Litho. 5754, 274 (2004).

[12] C. Rydberg et al., “Dynamic laser speckle as a detrimental phenomenon in optical projection lithography,” Journal of Microlithography, Microfabrication, and Microsystems, Vol 5, issue 3, (2006).
[13] T. Matsuyama et al., “An Intelligent Imaging System for ArF Scanner,” Proc. SPIE Adv. Litho. 6924, 63 (2008).
[14] P. Alagna et al., “Optimum ArFi laser bandwidth for 10nm node logic imaging performance.” Proc. SPIE 9426, Optical Microlithography XXVIII, 942609 (March 18, 2015); doi:10.1117/12.2085823.
[15] P. Alagna et al., “Lower BW and its impact on the patterning performance.” Proc. SPIE 9780, Optical Microlithography XXIX, 978008 (March 16, 2016); doi:10.1117/12.2219945.
[16] P. Alagna, et al., “Image contrast enhancement of multiple patterning features through lower light source bandwidth.” Proc. SPIE 10147, Optical Microlithography XXX, 101470N (March 30, 2017); doi: 10.1117/12.2263228.
[16] T. Sandstrom and C. Rydberg, “Sources and Scaling Laws for LEW and LWR.” Proc. of SPIE 6250, Optical Microlithography XX, 65200X (2007); doi: 10.1117/12.712248.
[17] O. Noordman, et al., “Speckle in optical lithography and the influence on line width roughness.” Proc. SPIE 7274, Optical Microlithography XXII, 72741R (2009); doi: 10.1117/12.814169.
[18] O. Kristun, et al., “Improving lithography pattern fidelity and line-edge roughness by reducing laser speckle,” 52nd EIPBN Conference (2008).
[19] C. Shin, “Variation-Aware Advanced CMOS Device and SRAM” Springer Series in Advanced Microelectronics 56 (2016)

DUV light source sustainability achievements and next steps

Yzzer Roman, Ted Cacouris, Kumar Raja Guvindan Raju, Dinesh Kanawade, Walt Gillespie,
Siqi Luo, Eric Mason, David Manley, Saptaparna Das
Cymer LLC (An ASML Company), 17075 Thornmint Ct., San Diego CA 92127

ABSTRACT

Key sustainability opportunities have been executed in support of corporate initiatives to reduce the environmental footprint and decrease the running cost of DUV light sources. Previously, substantial neon savings were demonstrated over several years through optimized gas management technologies. Beyond this work, Cymer is developing the XLGR 100, a self-contained neon recycling system, to enable minimal gas consumption. The high efficiency results of the XLGR 100 in a production factory are validated in this paper.

Cymer has also developed new light source modules with 33% longer life in an effort to reduce raw and associated resource consumption. In addition, a progress report is included regarding the improvements developed to reduce light source energy consumption.

Keywords: DUV ArF, Cymer, neon, recycle, sustainability, chamber

1. INTRODUCTION

Cymer continues to move ahead in developing its DUV light source technology and introduce initiatives for the platform that reduce the chipmaker operating costs, and business continuity risks. Significant resources and investment are dedicated for each of the next generation of improvements that include new algorithms [1] and new module technology [2]. Benefits for the chipmakers include lower cost of operation, higher system availability, and increased productivity. Consequentially, these initiatives have a positive impact on the environment as they reduce the light source environmental footprint as described in this paper.

2. SUSTAINABILITY ACHIEVEMENTS

The largest portion of light source operating costs was significantly lessened by the Cymer's neon reduction solution [1] introduced as neon shortages were putting at risk the chipmaker's business continuity. Further generations of neon reduction solutions continued to achieve additional savings while reshaping the semiconductor industry's demand for specialty gases [3]. Cymer light sources have achieved gas consumption of ~1,500 liters per billion pulse or 60 thousand liters per year for systems in high volume manufacturing (HVM). These efforts are described in detail in previous works [1] [2]. Further minimization of neon gas use is achieved through gas recycling as detailed in this paper and as described in previous works [2].

Light source consumption of helium gas has also been successfully reduced [4] and is on path for complete elimination from Cymer light sources. This helium use elimination requires innovations in the optical system design to account for its replacement with nitrogen. The introduction of nitrogen as a replacement for helium has been described in previous work [2]. Helium-free technology continues to advance as field deployment at chipmakers is proliferated.

Power saving has also been the focus of previous efforts when Cymer successfully introduced L3 chamber technology to decrease the power consumption by lowering the voltage curve [4]. Further improvements in the optical transmission as well as the deployment of L4 chamber technology are expected to reduce the overall consumption to 17% from the first generation of L3 chambers as described in this paper.

In aggregate, Cymer has introduced solutions that have achieved 50% reduction in the light source cost of operation, while new technologies support 80% reduction.

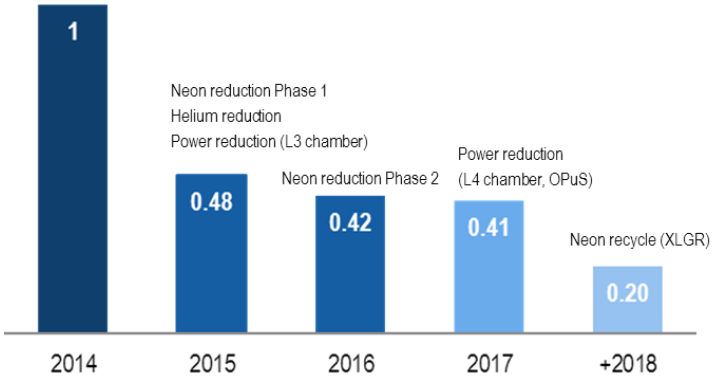

Figure 1 – Relative operational cost

3. NEON RECYCLE SYSTEM XLGR 100

XLGR 100 is the first neon recycle system for DUV ArF light sources deployed at a chipmaker. This recycle system allows reusing >90% of effluent gas, which would otherwise be released into the facility exhaust. The scrubbed neon-argon mix gas is captured by the XLGR for processing to ultra-high purity (UHP) specifications. This purified and reconstituted gas can then be introduced to the facility supply system as recycled gas.

A key feature of the XLGR is the ability to provide an uninterrupted gas supply to the connected light sources. The system features automatic controls that can select the gas source and switch between recycled and conventional supply depending on several factors. These factors can include system service event or when the recycled gas deviates from the programmed specifications. In these cases, the gas supply is automatically switched to the facility source.

Another key feature of the system is the ability to collect and supply recycled gas to multiple light sources. Since the recycled gas is required to meet Cymer gas specifications, it can be used across any connected light source. This feature allows for a flexible configuration that can function independent of the operation of connected light sources. Detailed XLGR recycle architecture has been described in previous work [2].

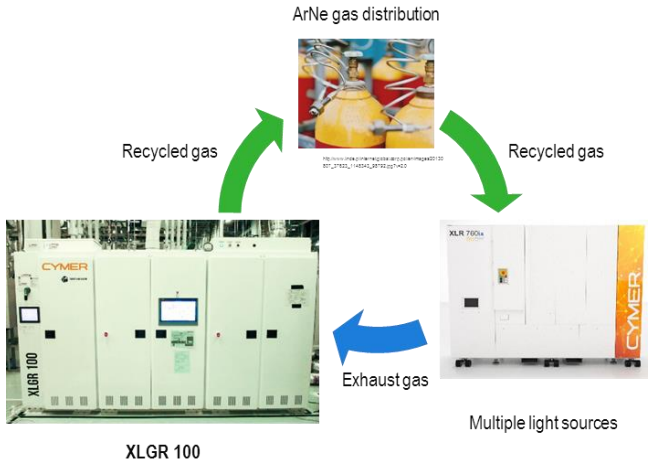

Figure 2 – Simplified schematic of recycled gas

The XLGR has been field deployed to a chipmaker and has been operating for over 120 days. During this period, the system has been proven highly efficient in maintaining the UHP gas specifications and removing other components that are not required for the lasing function of the light source. Argon and xenon, which are two critical components of the ArNe (bi-mix) gas blend, are required for efficient lasing and are maintained within the required levels as shown in the figures below.

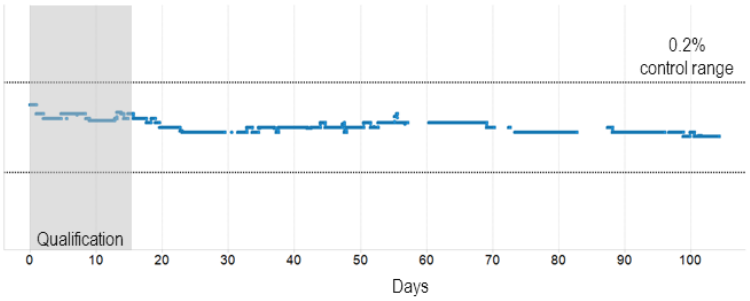

Figure 3 – Argon concentration (%) of the recycled gas

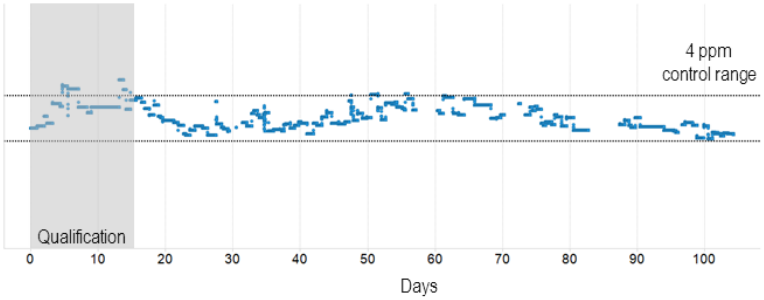

Figure 4 – Xenon concentration (ppm) of the recycled gas

4. LONG LIFE MODULES

Cymer successfully introduced the L4 advanced technology that extends the chamber life by 33% and improves its efficiency over the module life. This new technology introduced innovative materials that reduce the life-limiting factors of the chamber and provide better efficiency via reduced voltage profile. Chipmakers continue to propagate the L4 chamber throughout their fabs to increase light source availability and further productivity from reduced module replacements at service events. Over 250 L4 chambers have been field deployed and continue to provide excellent performance results. Cymer will continue its efforts to develop future module technologies that will provide a 2x increase in module life from the first generation of L3 chamber technology.

As the service intervals continue to extend, additional technology developments are required on optical modules to support the longer intervals. Therefore, Cymer developed improved optic modules that can last longer while providing stable performance and predictable life. The next figure shows the improved modules as located in the light source.

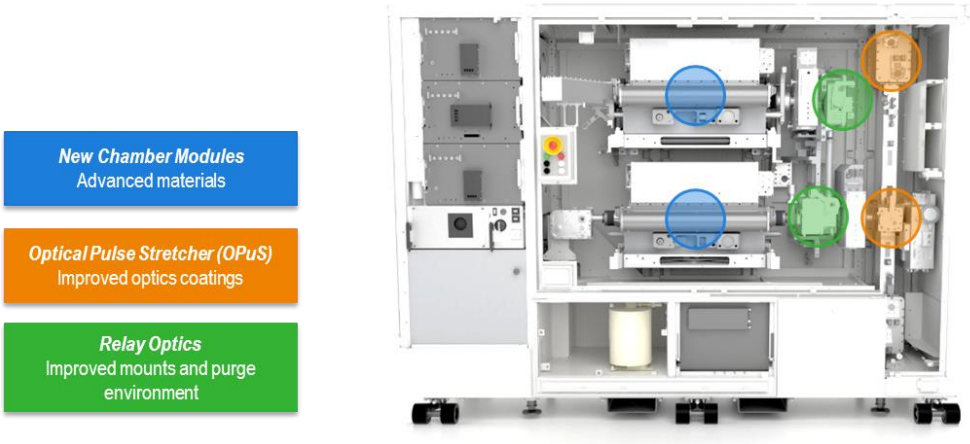

Figure 5 – Improved modules for XLR platform

The L4 chamber also provides two main benefits that directly translate to reduced carbon footprint:

1. Longer replacement interval means reduced service events and their associated environmental impact
2. Improved design in new modules increases overall system wall-plug efficiency (input to output power ratio)

The module lifecycle starts when the raw metals are produced and ends when the materials are recycled. Therefore, reduced service events means that fewer modules need to be manufactured and shipped to chipmakers. Since raw metal production is an inherently energy intensive process [5] [6], a significant reduction in the carbon footprint is possible by fewer material requirements. Despite significant improvements over the years in transportation efficiency, a large amount of fuel continues to be spent and carbon emissions to be produced in the shipment of modules [7]. Moreover, less materials need to be recycled at the end of the module's life. By continuing to reduce the overall number of modules, reduction across all of these steps in the module lifecycle can be realized.

The benefits from efficiency improvement and reduced power consumption will be discussed in the following section of this paper. Additionally, an estimated carbon footprint reduction roadmap will be presented in the section thereafter.

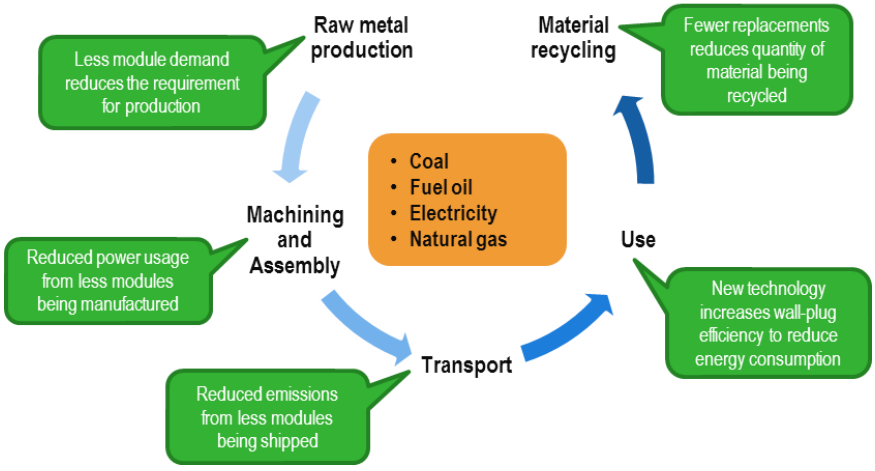

Figure 6 – Module lifecycle

5. ENERGY CONSUMPTION

Reduction in power consumption results from the advanced technology and new materials that allow to lower the power demand to achieve the same gain level. This is accomplished via the lower voltage profile over the life of the chambers. Cymer first introduced the patented movable electrode technology in the L3 chambers [8]. Further improvements to the chamber materials and configuration achieved a 15% net reduction in power consumption from a 50% reduction in voltage slope. With the introduction of the new L4 technology, a net 17% power reduction can be achieved. An average voltage curve for L4 was composed from the >250 chamber population deployed at chipmakers and is shown below.

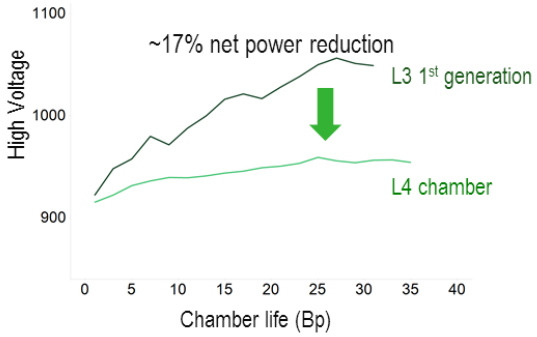

Figure 7 – Voltage curve evolution from L3 to L4 chambers

New optical materials developed for the Optical Pulse Stretcher (OPuS) have initial higher transmission efficiency and also a reduced loss over the life of the modules. The OPuS is located at the exit beam of the amplifier cavity and is the last optical module before delivering the beam. The life of the module is increased by 1.7x from these improvements as the threshold for module replacement is not reached until a significant amount of pulses later. Decreasing the transmission losses over time in the amplifier cavity reduces the input power requirements to maintain the same level of energy output.

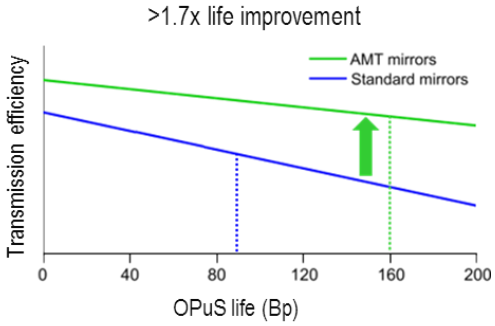

6. CO2 EMISSIONS

As new modules technologies are developed, time interval in between service events continues to extend as a result of module lifetime increase. A light source using L3 chamber technology would experience one service event every 9 months. The new L4 chamber technology enables for one service event per year, a 33% increase in lifetime. Future technologies currently in development will continue prolonging the service events out to 20 months, or 0.6 service events per year. Fewer demand and production of chambers results in removing the associated energy requirements across the entire module lifecycle that includes metal production, shipping, and recycling as described in Section 4. An estimate of the carbon footprint is calculated using publicly available studies that included carbon values for metal procurement and production [5] [6] [9], machining [10], and air transport [7].

Power reduction during the life of the chamber is also achieved by the new technologies. The power savings resulting from the L3 chamber were estimated to approximately 33,600 kilowatt-hours per year. The cumulative reduction of 40,700 kilowatt-hours per year is due to the L4 chamber and new Optical Pulse Stretcher. Improvements in future generations will continue to reduce the power consumption of the light source. A carbon footprint is also calculated from readily available data [10] on the emissions from different energy producing methods.

An corresponding benefit to reducing the service events is the increase in system availability that can then be used for production. Using a nominal lithography scanner productivity, an estimate of the additional wafer passes is calculated. The additional production estimate from moving from L3 to L4 technology, or extending the service from 9 to 12 months, is 1,620 wafer passes per year. As the next technology is introduced and the service interval keeps extending, there is an additional productivity increase.

The chart below describes the 28% carbon footprint reduction resulting from a service events by 50% and by the power savings from each of the technologies presented. This environmental footprint reduction is complemented by the increase in productivity, therefore, the carbon can be calculated per each wafer pass.

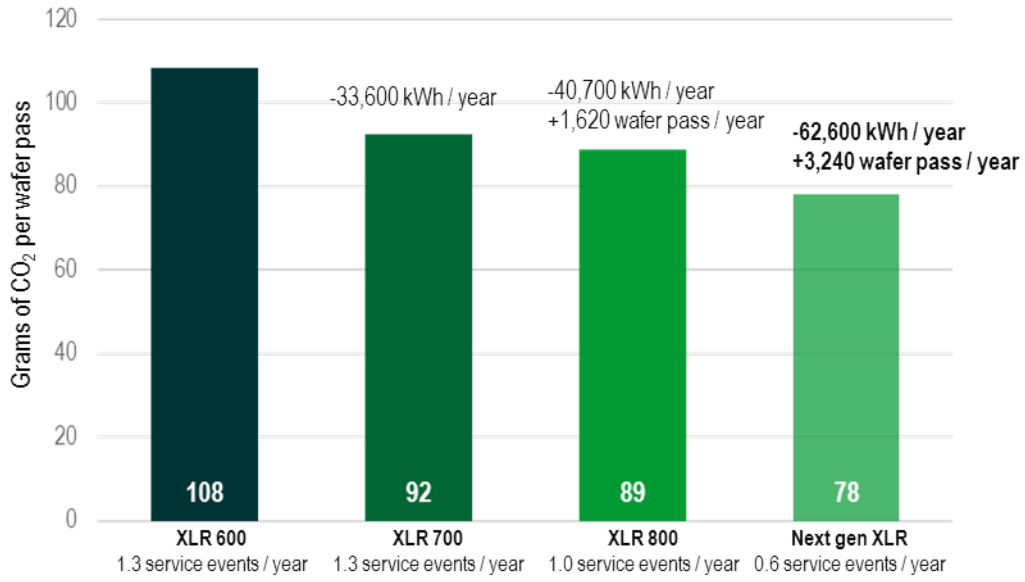

7. CONCLUSION

Cymer continues to develop cutting edge technology for the DUV light source platform that is focused on increasing system availability and reducing the dependency on rare and non-renewable resources. The neon recycle system, XLGR 100, has proven its ability to produce UHP gas and reduce the dependency of traditional semiconductor gas sources. Similarly, the L4 chamber has successfully extended the service intervals for HVM customers and enabled one service event per year. Direct benefits for chipmakers from these programs are reduced operating costs and increased productivity. Consequentially, these initiatives have a positive impact on the environment by reducing the environmental footprint of each wafer pass by using less energy and resources.

8. REFERENCES

[1] D. Kanawade, Y. Roman, T. Cacouris, J. Thornes and K. OBrien, "Neon Reduction Program on Cymer ArF Light Sources," *SPIE - Optical Microlithography XXIX*, vol. 9780, 2016.

[2] Y. Roman, D. Kanawade, W. Gillespie, S. Luo, M. Thever, T. Duffey, K. O'Brien, R. Ahlawat, A. Dorobantu, E. Gross and E. Mason, "Advances in DUV light source sustainability," *SPIE - Optical Microlithography XXX*, vol. 10147, 2017.

[3] R. Betzendahl, "The ever-changing rare gas market," *Specialty Gas Report*, 1 12 2017.

[4] E. Gross, G. G. Padmabandu, R. Ujazdowski, D. Haran and e. a. Matt Lake, "Enabling CoO improvement thru green initiatives," *SPIE - Optical Microlithography XXVIII, 942626*, vol. 9426, 2015.

[5] Energetics, Incorporated, "Energy and environmental profile of the US iron and steel industry," U.S. Department of Energy - Office of Industrial Technologies, Washington DC, 2000.

[6] A. Hasanbeigi, L. Price, N. Aden, C. Zhang, X. Li and F. Shangguan, "A comparison of iron and steel production energy use and energy intensity in China and the U.S.," Ernest Orlando Lawrence Berkeley National Laboratory, 2011.

[7] Cathay Pacific, "Cathay Pacific sustainable development report 2015," 2015.

[8] R. Sandstrom, T. Chung and R. Ujazdowski, "Extendable electrode for gas discharge laser". United States of America Patent US 8,526,481 B2, 3 09 2013.

[9] J. Stubbles, "Energy use in the US steel industry: A historical perspective and future opportunities," US Department of Energy - Office of Industrial Technologies, Washington DC, 2000.

[10] US Environmental Protection Agency, "Greenhouse gases equivalencies calculator," 2016. [Online]. Available: https://www.epa.gov/energy/greenhouse-gases-equivalencies-calculator-calculations-and-references. [Accessed 1 February 2018].